Surface texture modifications for oral processing applications

Taylor, Brogan L.; Mills, Tom B.

DOI:
10.1016/j.biotri.2020.100132

Document Version
Peer reviewed version

Citation for published version (Harvard):
Taylor, BL & Mills, TB 2020, 'Surface texture modifications for oral processing applications', *Biotribology*, vol. 23, 100132. https://doi.org/10.1016/j.biotri.2020.100132

Surface texture modifications for oral processing applications

Brogan L. Taylor[1], Tom B. Mills[1]

[1]School of Chemical Engineering, University of Birmingham, Birmingham, B152TT

Key words: oral processing; particulate suspensions; surface texture; biotribology.

Abstract

The surfaces currently used in soft tribology when assessing oral processing *in-vitro* are not yet fully representative of the oral cavity. Surface topography, among other physical and chemical qualities, plays a key role in determining friction properties. This work examines the friction properties of pillar textures of 500 μm and 1000 μm in polydimethylsiloxane that resemble papillae found on the human tongue. Initially a system with Newtonian fluids was investigated using these textured discs. It was found the area density of pillars affected hydrodynamic lubrication, with a greater area density promoting full film lubrication. Model hard, spherical particulate suspensions were also examined showing a reduction in friction coefficient so long as particles were smaller than the pillars; particles that were too large for the cavities increased friction. Soft, deformable particulate gels, commonly used in food products, demonstrated different behaviour to the hard particulate systems. The findings show great potential for a more realistic analysis of complex food formulations and understanding of their behaviour as they are processed in the mouth, although a number of other factors still need to developed.

1. Introduction

As food enters the mouth and is consumed, it is subjected to a series of mechanical processes by the lips, tongue, teeth and palate in order to facilitate digestion. The surface of the tongue comprises of macroscale pits and grooves due to the presence of papillae. This design increases the contact area between surfaces and food allowing control of processing in the oral cavity. Papillae on the human tongue are commonly divided into four types: the folate and vallate which are located in the posterior of the tongue, and the fungiform and filiform papillae; located on the anterior. Papillae range in size and shape but typically have a height and diameter under 1 mm [1–3]. Mechanoreceptors found on the interface of oral surfaces, including the tongue, allow the perception of friction of the food. Friction in the mouth is believed to contribute to mouthfeel attributes including creaminess, roughness and detecting the presence of particles [4]. The friction properties depend on many factors including the lubrication properties of saliva, the oral surfaces involved (which differ between individuals depending on age, sex, health etc.) and the food itself. Studies have shown tribology to be a promising technique for correlations with oral behaviour and sensory perception, specifically relating to squeeze flow between the tongue and palate [5]. Quantitative friction and lubrication properties combined with other physical measurements such as rheology and texture analysis as well as sensory perception measurements give an increased understanding of oral processing [4]. Researchers continue to study and link rheology, sensory properties and tribology as investigations continue into understanding and relating tribological measurement to the oral perception of food and drink products [2,6–10].

A range of soft materials have been used in tribological oral processing applications including rubbers, silicones and biological tissues [11,12]. These materials typically fail to represent the inherent structural intricacies and topography of the tongue which are expected to affect friction. A number of studies address this by investigating rough soft contacts [11,13–16]. Krzeminski *et al.* found lubricating performance was strongly affected by patterning on the tribological testing surface, where the roughness indices were more crucial for lubricating properties in a tribosystem than the stiffness of the material [17]. A study by Selway, Chan, & Stokes proposes the mechanism of lubrication within a smooth contact is governed by localised fluid entrapment and interfacial

viscoelastic effects, whereas a different mechanism occurs for rough contacts where the lubricant properties have less effect on the interfacial friction [18]. Other studies look to more closely resemble the tongues surface including Nguyen *et al.* who studied three solid substrates: surgical tape, silicone rubber and ethylene propylene diene monomer rubber [19]. It was observed that surgical tape best discriminated dairy solutions of different compositions compared to the rubber substrates. The authors attribute this to the surfaces being similar to that of the tongue. None of these surfaces were as representative of the tongue's architecture as the study by Dresselhuis *et al.* who used oral tissue in the form of a cross section of pig tongue *ex vivo* [12]. However, using a biological sample may cause issues in reproducibility, and samples may not be available or accessible to all researchers, so the design of textures using a non-biological material that are of the same order of magnitude of the tongue is of interest. Ranc *et al.* investigated a range of hemispherical surface structure in the sub-millimetre range, corresponding to typical tongue roughness [20]. They found the textures critically affected the frictional behaviour of the systems tested. Under dry conditions, the coefficient of friction decreased significantly with an increase in density of hemispherical pillars. In lubricated systems, a structure of high pillar density yielded higher coefficients of friction. This effect was attributed to the protruding structures disturbing the homogeneity of the lubricant film.

Whilst considering the complexity of replicating the human tongue, it is also important to consider that foods products are structurally complex, comprising of multiple components, systems and phases. Food products are often particulate in nature but few tribological studies examine particulate samples directly. One example of these is Yakubov *et al.* who investigated glass spheres in glycerol [13]. In this study, the authors varied the viscosity of the matrix in order to probe the influence of particles across all lubrication regimes. In the boundary regime, particles lowered friction due to ball bearing behaviour providing surface roughness was low enough to prevent surface-asperity interactions. A study by Liu *et al.* reported a similar ball bearing lubrication mechanism from the presence of micro-particulated whey protein particles reduced friction [22]. Chojnicka-Paszun & De Jongh investigated suspensions of microcrystalline cellulose particles [23]. The researchers found the particles may not fit into surface asperities, so enhanced surface roughness affording an extended boundary regime.

75 Ideally, more work on particulate suspensions should be completed to understand how they lubricate
76 between contacting soft surfaces that are in relative motion.

77 This study aims to examine the influence of surface texture on the lubrication properties of particulate
78 suspensions relevant to oral processing applications. Soft-surface textures and particles have been
79 investigated tribologically, but very few studies examine these together, despite it being known
80 particles interact with oral surfaces to affect sensory perception [24–26]. It is clear from existing
81 research that lubrication mechanisms for soft contacts are affected by surface roughness or textures
82 and continued research in this area is necessary to understand the relevance to oral processing
83 [18,19,27]. Existing texture studies are typically on the micro- or nano-scale, whereas this study aims
84 to more closely resemble the tongue structure by investigating larger (>500 μm) textures. Model hard
85 spherical particles are investigated as well as soft, deformable particulate systems in order to examine
86 a range of particle systems that may occur in food products. Typically, protein or polysaccharide
87 suspensions are investigated; in this study agar fluid gels were used as these form relatively large
88 particles and are more frequently being used in food products as fat replacement [28–31].

89 ## 2. Materials and methods

90 ### 2.1. Materials

91 Glycerol >99% and agar were obtained from Sigma Aldrich, UK. Microcrystalline cellulose (Viva Pur
92 MCC Spheres range) was kindly provided by JRS Pharma, Germany. Sylgard 184 Silicone Elastomer
93 kit was purchased from Dow Corning. Materials were used with no further modifications or
94 purification.

95 #### 2.1.1. Glycerol solutions

96 Glycerol solutions of 25%, 50% and 75% glycerol were prepared by dispersing the desired wt% of
97 glycerol in distilled water under stirring. Solutions were stirred for at least one hour to ensure
98 thorough dispersion.

2.1.2. Hard particle suspensions

Hard spherical, microcrystalline cellulose particles (MCC) were added to glycerol under stirring at a phase volume of 10% w/v (unless stated otherwise). Suspensions were stirred for at least one hour to ensure uniform dispersion. Two discrete particle sizes with a bulk density of 0.8 gcm^{-3} were used for this study: 100-200 μm (Viva Pur MCC Spheres 100) and 500-700 μm (Viva Pur MCC Spheres 500).

Particle size distribution was measured using an optical laser particle size analyser (Mastersizer, Malvern Instruments, UK) and are summarised in *Table 1,* below. Measurements were carried out in triplicate.

Table 1 - A table showing median diameter of microcrystalline cellulose particles.

Particle type	**Median diameter of particle (μm)**
100-200 μm	158 ± 1
500-700 μm	536 ± 3

2.1.3. Soft particle suspensions

Agar fluid gels were prepared in a lab-scale continuous process pin-stirrer. The required mass of agar was dispersed in deionised water and heated to 90 °C whilst stirring. The resultant hot solution was fed through a peristaltic pump into a jacketed pin-stirrer cooled to 5 °C. The inlet temperature was controlled to ~ 70 °C and the outlet to 5 °C to ensure gelation occurred under shear (gelation temperatures ~ 30 °C). The speed of the pump was set to 25 mL min^{-1}. The shaft rotation speed was set to 2000 rpm. Fluid gels were stored at 5 °C until use.

To determine the diameter of the agar fluid gel particles, particles were analysed using an optical laser particle size analyser (Mastersizer, Malvern Instruments, UK) and are summarised in *Table 2,* below. Measurements were carried out in triplicate.

Table 2 – A table showing median diameter of agar fluid gel particles.

Concentration of agar (wt%)	**Median diameter of particle (µm)**
2	135 ± 5
4	121 ± 2

2.2. Methods

2.2.1. Shear rheology

Rheological measurements were performed using a Kinexus Pro rheometer (Malvern Instruments, UK). For glycerol suspensions, viscosity curves were obtained through a range of applied shear rates at equilibrium (1–100 s^{-1}) using a cup and bob geometry at 25 °C. For MCC particulate suspensions, viscosity curves were obtained by recording shear viscosity through a range of applied shear rates at equilibrium (1–100 s^{-1}) using a spiralled cup and bob geometry at 25 °C. For agar fluid gels, measurements were completed at 25 °C, 48 hours after production, to ensure sufficient post-production particle ordering. Viscosity curves were obtained by recording shear viscosity through a range of applied shear rates at equilibrium (0.001–500 s^{-1}) using a serrated parallel plate geometry (60 mm serrated parallel plate) with 1 mm gap at 25 °C. Experiments were carried out in triplicate.

2.2.2. General tribological set up

A mini traction machine (MTM) manufactured by PCS Instruments, UK was used to perform tribological measurements. A sample size of 15 ml with volume reducing insert fitted was used in all cases. For each experiment, the tribopair consisted of a 0.019 m diameter stainless steel ball (supplied by PCS Instruments, UK) and polydimethylsiloxane (PDMS) disc. PDMS was chosen as the disc material due to its wide use in soft-contact tribology and its surface properties can be easily tailored (surface topography and hydrophobicity) [11,23,31,32]. Prior to testing, surfaces were sonically cleaned in isopropanol followed by distilled water for 6 minutes each.

2.2.3. Mould preparation

A moulding-casting technique was used to create the PDMS discs. Moulds were created using AutoCAD software and the Form Labs Form2 3D printer. The advantages of using this method to create moulds are that it is efficient for time and resources. Most importantly, however, the moulds are easily designed on the software allowing for a range of surface structures to be explored. Moulds to cast discs of 46 mm diameter, 4 mm thickness suitable for use in the MTM were printed using Grey Resin V3 supplied by Formlabs. Once printed, moulds were sonically cleaned in isopropanol to remove any excess uncured resin. The first PDMS disc was disposed of to ensure any uncured resin did not affect the disc surface.Six surfaces were investigated: S0, a smooth disc with no textures added to the mould (average roughness, $S_a \approx 2$ µm, characterised using a KLA Tencor MicroXAM2 Interferometer), and E1, E2, E3, E4 and E5 each with cylindrical pillar cavities of varying diameter, height and density, summarized in *Table 3* below, that are a similar size range to papillae found on the human tongue [1]. Classical Hertz contact theory was used to calculate the contact area and maximum contact pressure [33]. The contact radius (A_r) subject to load (W) is given in Equation 1:

$$A_r = \left(\frac{3WR^*}{4E^*}\right)^{\frac{1}{3}} \quad (1)$$

$$R^* = \left(\frac{1}{R_1} + \frac{1}{R_2}\right)^{-1} \quad (2)$$

$$E^* = \left(\frac{1-v_1^2}{E_1} + \frac{1-v_2^2}{E_2}\right)^{-1} \quad (3)$$

$$P_{max} = \frac{3}{2\pi A_r^2} \quad (4)$$

R* and E* are the reduced radius and reduced elastic modulus, given by Equation 2 and 3, where the subscript numbers 1 and 2 denote the two contacting surfaces e.g. 1 = ball and 2 = disc. R_1 and R_2 are the radii of the contacting surfaces, E_1 and E_2 represent elastic moduli and ν_1 and ν_2 are the Poisson's ratios. The maximum pressure in the contact can be calculated by Equation 4. In the case of this set up, E* = 170 MPa, R* = 0.0095 m, Ar = 2.3 mm, W = 3 N, and the maximum contact pressure = 270 kPa. The maximum pressure in the contact is an order of magnitude higher than the pressure of the

oral-palate contact of healthy adults (typically around 30 kPa). For these pressures to be achieved, the tribological set-up would require using loads lower than 0.1 N, which is not possible when using a MTM [2].

Water contact angle measurements were performed to assess wettability of the PDMS substrates (*Table 3*). Sessile drop contact angle measurements were performed using a goniometer (Krüss Drop Shape Analyser, Germany). A symmetrical drop of volume of 10 µL was deposited on the surface material using a syringe. All surfaces were cleaned with ethanol, distilled water and dried in air prior to testing. The contact angles were determined at room temperature from image analysis via the Laplace-Young method using DSA Software provided with the equipment. Reported contact angles are the average of three measurements. All textured surfaces (E1-E5) show similar hydrophobicity.

Table 3 – A table showing surface properties the four fabricated PDMS discs: S0, E1, E2, E3, E4 and E5 with varying cylinder diameter, height and area density.

	Cylinder diameter (µm)	**Cylinder height (µm)**	**Cylinder density (mm^{-2})**	**Area coverage of cylinders (%)**	**Theoretical no. of cylinders in the contact**	**Water contact angle (°)**
S0	-	-	0	0	0	102 ± 3
E1	500	500	0.5	10	8	142 ± 5
E2	500	500	1	20	16	146 ± 2
E3	1000	1000	0.25	20	4	151 ± 6
E4	500	500	2	40	32	147 ± 6
E5	1000	1000	0.5	40	8	146 ± 6

2.2.4. Disc fabrication

The discs were made from PDMS, using Sylgard 184 Silicone Elastomer kit. The two components (silicone elastomer and curing agent) were mixed in the recommended 10:1 ratio. The binary liquid mixture was poured into the 3D printed mould, degassed and placed in an oven at 60 °C for 3 hours. Without removing the disc, the moulds were left to cool for at least 24 hours. The discs were the

removed and stored in an airtight container before use. The Young's Modulus of the discs was 1.3 ± 0.2 MPa. Each disc was used once before disposal. The outcome is shown in *Figure 1* below.

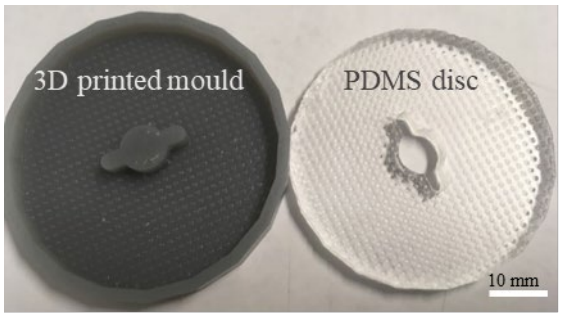

Figure 1 – 3D printed mould in Grey Resin (Formlabs), left, and PDMS disc (46 mm diameter, 4 mm thickness), right, cast from the mould for use in a mini traction machine.

Surfaces were analysed before and after testing where cylinders remain intact and no visible damage to the structure or shape was observed, as can be seen in optical microscopy images (obtained using Leica Microsystems, UK with objective lens up to 4× magnification) shown below in *Figure 2*.

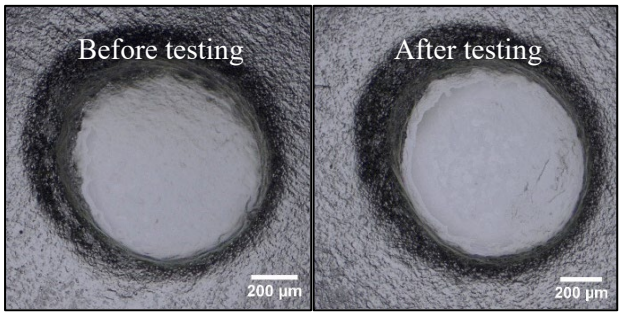

Figure 2 – light microscopy images of 1mm cylindrical pillars before (left) and after (right) testing.

2.2.5. Newtonian systems

Glycerol was used as the lubricant due to its Newtonian behaviour and aqueous glycerol solutions were used to probe the effect of viscosity and fluid substrate-interactions. Tribopairs of PDMS disc and stainless steel ball were used with six different surfaces: S0, E1, E2, E3, E4 and E5. The testing conditions used were 50% SRR and entrainment speed 1 to 1000 mm/s. Six Stribeck sweeps were

performed alternating between ascending and descending speed without unloading for each step at room temperature (25 °C) at normal force 3 N. Tests were performed in triplicate to obtain an average.

2.2.6. Particulate systems

Glycerol and MCC particle dispersions and agar fluid gel particles were studied. A PDMS disc with textured surface and steel ball were used. The testing conditions used were 50% SRR and entrainment speed 1 to 750 mm/s. Six Stribeck sweeps were performed alternating between ascending and descending without unloading for each step at room temperature (25 °C) with normal force 3 N. Tests were performed in triplicate to obtain an average.

3. Results and discussion

3.1. Influence of surface texture with Newtonian systems

Aqueous solutions of glycerol were used to assess textured PDMS surfaces. *Table 4* lists the glycerol solutions used in this study and their measured viscosities at 25 °C. All samples demonstrated Newtonian behaviour across the shear rates tested. The lubricating properties were measured using steel ball and textured PDMS discs: S0, E1, E2, E3, E4 and E5 at 3 N normal force, 50% SRR.

Table 4 – Table showing measured viscosity with cup and bob geometry averaged across 1-100 s^{-1} for glycerol solutions at 25 °C.

Glycerol (wt%)	**Viscosity at 25 °C (Pa s)**
25	0.0016 ± 0.0002
50	0.0038 ± 0.0003
75	0.0249 ± 0.0004
100	0.90 ± 0.01

Stribeck curves were constructed (*Figure 3)* for surfaces and the glycerol solutions to examine fluid substrate interactions, with data for overlapping speeds omitted for clarity. At 0.1 Pa mm, the

boundary regime is generally observed for all surfaces. As speed increases, the onset of the mixed regime occurs first for E5, E2, E4 and S0 and then E1 and E3. For boundary and the onset of the mixed regime, surfaces E2 and E5 showed a lower friction coefficient. The textured surfaces transition into the elastohydrodynamic (EHL) lubrication regime at a lower speed compared to S0, with the greater area density of pillar cavities transitioning earlier. S0 transitions over a short speed range from boundary lubrication as speed increased to mixed and EHL lubrication. In comparison, the textured surfaces show extended mixed lubrication regimes. S0 also shows the lowest friction coefficient above 1 Pa mm as the transition to EHL occurs, with all textured surfaces demonstrating a higher friction coefficient at higher speeds. At 1000 Pa mm, S0, E1, E2 and E3 tend to similar friction coefficient values; whereas E4 and E5 tend to a similar, greater friction coefficient.

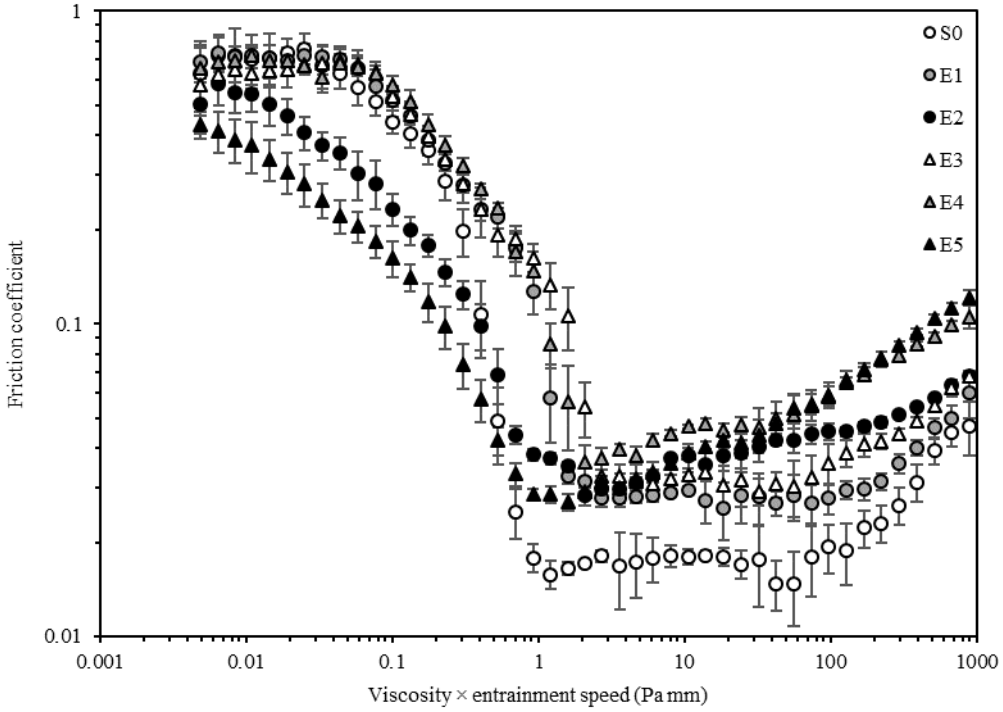

Figure 3 – Stribeck curves showing friction coefficient versus entrainment speed as a function of viscosity for glycerol suspensions with non-textured (S0) and textured PDMS surfaces (E1, E2, E3, E4 & E5).

It is clear the textured surfaces affect friction across all regimes. As the textured surfaces transition to the EHL earlier than S0, the pillar cavities are proposed to act as wells or reservoirs of lubricant which

236 are able to facilitate lubrication at high speeds by providing a continuous supply of lubricant even as
237 greater hydrodynamic pressure is applied as speeds increases [34,35]. Therefore, at high speeds the
238 viscous drag from the lubricant is greater for the textured surfaces with the higher area density and a
239 higher friction coefficient is observed (*Figure 4*).

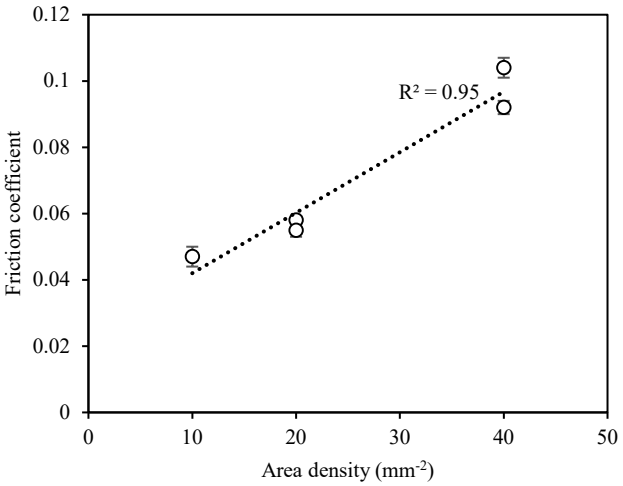

240

241 *Figure 4 – Friction coefficient versus area density of pillars at 500 Pa mm.*

242 ### 3.2. Influence of surface texture with particulate suspensions

243 Food formulations are often particulate in nature therefore the aim of these experiments was to
244 investigate the friction properties of particulate suspensions on the textured PDMS surfaces.

245 #### 3.2.1. Hard particle dispersions

246 Model particulate suspensions of glycerol containing 10% phase volume of rigid, spherical MCC
247 particles were examined. The shear rheology was measured and frictional behaviour assessed using
248 the MTM, as described in Section 2.2. A tribopair of stainless steel ball and PDMS discs were used.
249 Three surface textures were investigated: S0, E2 and E3. All particle dispersions showed Newtonian
250 behaviour over the speed range tested, with measured viscosities described in *Table 5*.

Table 5 - Table showing measured viscosity with spiral cup and bob geometry averaged across 1-100 s^{-1} for glycerol solutions at 25 °C.

Glycerol and particle dispersion	Viscosity at 25 °C (Pas)
No particles	0.90 ± 0.01
100-200 µm	0.91 ± 0.01
500-700 µm	0.92 ± 0.02

Figure 5a shows the friction coefficients of the glycerol suspensions measured using the non-textured PDMS disc, S0. At the initial stages of the lubrication process (for entrainment speeds up to 10 mm/s) the friction coefficient of the three systems decreased with increasing speed indicating mixed lubrication. The particulate systems showed greater friction coefficient below 10 mm/s compared to glycerol alone showing particles are influencing the friction response at low speeds when surfaces are likely to be in contact. As speed increases, clear distinction between no particle and particle suspensions was observed. Both the particle suspensions showed a similar, greater friction coefficient in EHL regime.

Figure 5b shows the friction coefficients measured from glycerol suspensions with textured surface E2 with cylindrical pillars of 500 µm height and diameter. For speeds lower than 10 mm/s, the addition of particles increased the friction coefficient as with surface S0. As speed increases and mixed lubrication transitions to EHL, the friction behaviour of the particulate suspensions differs. The particles sized 100-200 µm show a lower friction coefficient, with values closer to glycerol alone, compared to larger 500-700 µm particles.

Figure 5c shows the friction coefficients measured from glycerol and glycerol particulate suspensions with textured surface E3 with cylindrical pillars of 1000 µm height and diameter. For particles suspensions at speeds lower than 10 mm/s, the friction coefficient was higher than glycerol without particles, observed with surfaces S0 and E2. As speed increases, the friction response for all samples

was similar and a smaller difference between the samples was observed compared to surfaces S0 and E2.

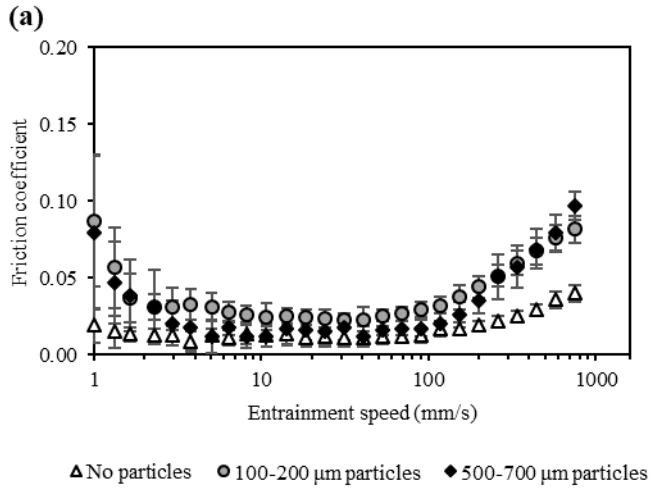

274

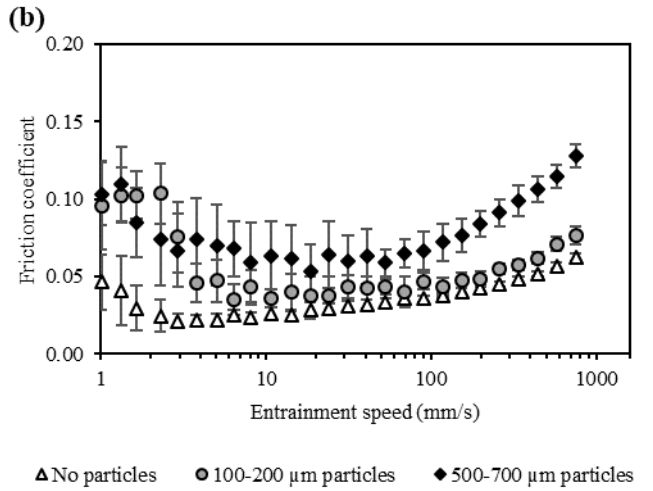

275

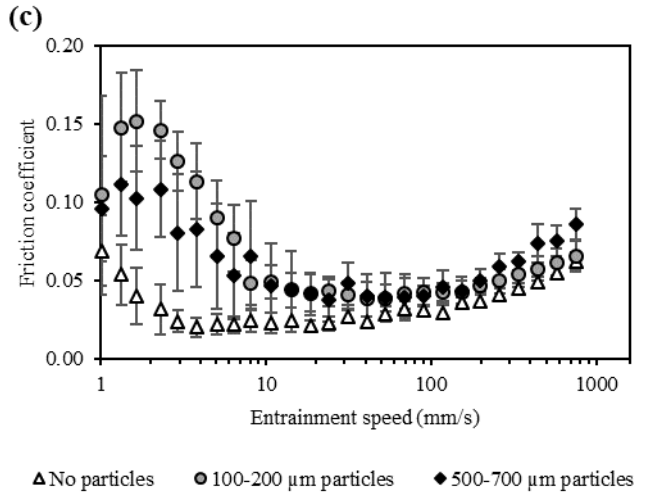

276

277 *Figure 5 - friction coefficient versus entrainment speed for glycerol suspensions containing 10%*

278 *MCC particles, with pure glycerol for comparison with surfaces S0 (a), E2 (b) and E3 (c).*

To compare how the particulate systems behave across different surfaces, the surfaces were compared for a given particle size. For no particles, the results are presented in *Figure 6a*.

For the 100-200 μm MCC particles in the boundary regime (< ~10 mm/s) (*Figure 6b*), smooth surface S0 has the lowest coefficient of friction and surface E3 has the highest. As speed increases and the mixed and EHL regimes are entered, the surfaces behave similarly, however, the particulate systems show a lower friction coefficient with the textured surfaces E2 and E3 compared to smooth surfaces S0. The textured surfaces act to elongate the mixed lubrication regime as surface S0 enters the EHL regime around 100 mm/s, E2 around 200 mm/s, and E3 around 300 mm/s.

For MCC particles sized 500-700 μm (*Figure 6c*), S0 also has the lowest coefficient of friction below speeds of 8 mm/s and the textured surfaces showed a higher friction response. As speed increased above 75 mm/s, surface E2 shows the highest friction response. Here, 500-700 μm particles are too large to fit into the 500 μm features in the surface. However, as the EHL regime is entered above 100 mm/s, S0 and E3 show similar friction behaviour. Particles are expected to fit into 1000 μm cavities on surface E3 which in turn has shown a reduced friction coefficient in this system compared to E2.

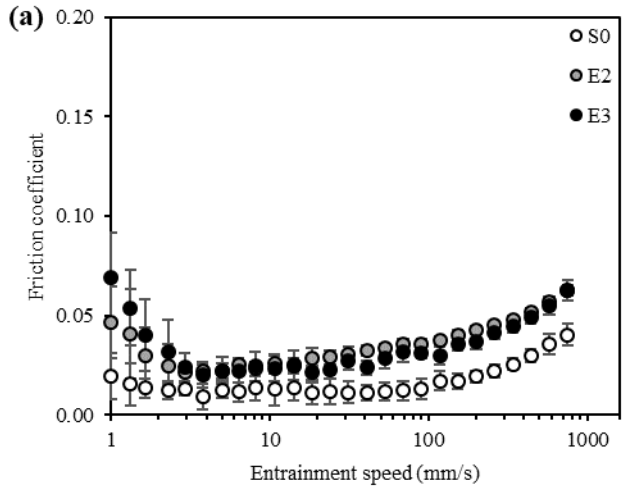
(a)
0.20
0.15
0.10
0.05
0.00
Friction coefficient
1
10
100
1000
Entrainment speed (mm/s)
S0
E2
E3

294

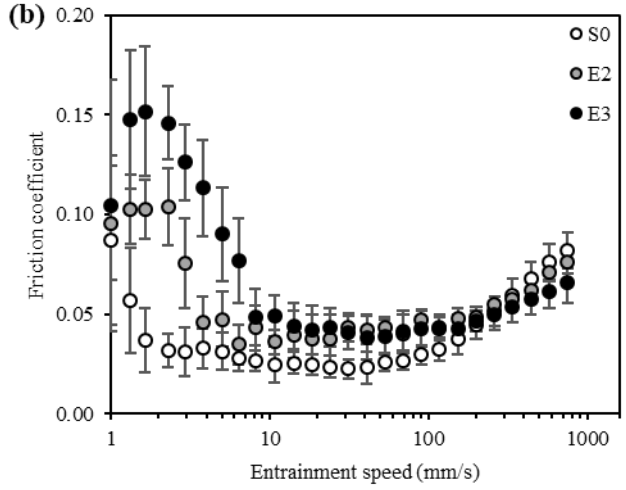
(b)
0.20
0.15
0.10
0.05
0.00
Friction coefficient
1
10
100
1000
Entrainment speed (mm/s)
S0
E2
E3

295

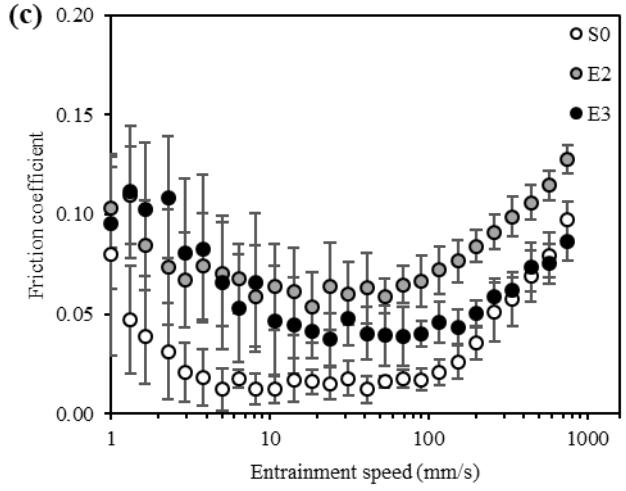
(c)
0.20
0.15
0.10
0.05
0.00
Friction coefficient
1
10
100
1000
Entrainment speed (mm/s)
S0
E2
E3

296

Figure 6 - friction coefficient versus entrainment speed for textured surfaces with glycerol suspensions without particles (a), with particles sized 100-200 µm (b) and with particles sized 500-700 µm (c).

In general, these results show the addition of particles results in higher friction. In this study, the particles used are relatively large and it is expected they are larger than the gap between the contacting PDMS and steel surfaces. However, due to the deformable nature of the soft PDMS surface and the consequential large contact area, it is clear from the data (independent of surface texture) particle suspensions are entrained between the contacting surfaces and influence friction, even at low speeds when the gap between contacting surfaces is expected to be small. This agrees with a previous study which showed hard particles directly interacted with the surface and were present even at low entrainment speeds attributing this to the deformable nature of the contact [23]. When surfaces are compared for a given particle size, it becomes clear particles act to reduce the friction coefficient with the textured surfaces in the EHL regime, so long as they are able to 'fit' inside cavities. This reduction in friction has also been observed at the smaller length scale when particles were able to fit inside asperities [21,23,31].

To understand the lubrication of the particles further, the role of phase volume was examined as both particles and the continuous phase are expected to affect friction and lubrication properties [28,36]. *Figure 7a* shows friction coefficient versus particle phase volume of MCC particles sized 100-200 µm at 750 mm/s where friction properties are expected to be dependent on the bulk properties of the lubricant (EHL regime). As phase volume of particles increases, friction coefficient increases for all surfaces investigated. The surface has little impact on friction coefficient at phase volumes greater than 10% with overlap of standard deviations showing similar friction response. Below 5% phase volume of particles for surface S0, the friction coefficients are lower than for the textured surfaces E2 and E3. It is likely due to a continuous film lubricating between the ball and the smooth surface that is not interrupted by surface textures or particles in the contact (as there are fewer particles in suspensions) [28,36]. Above 10% particle phase volume, the friction response of the surfaces is similar showing the particles are dictating friction response.

Figure 7b shows friction coefficient versus particle phase volume of MCC particles sized 500-700 µm at 750 mm/s. As phase volume increases, the friction coefficient increases for all surfaces increased. Surfaces S0 and E3 behaved similarly, whereas the friction coefficients for surface E2, with cylindrical pillars of 500 µm height and diameter, are consistently greater than E3, regardless of the amount of particles added. The particles are not able to fit into the pillars of surface E2 unlike surface E3 demonstrating that if the particles are able to fit inside the pillar cavities, a lower in friction coefficient can be observed.

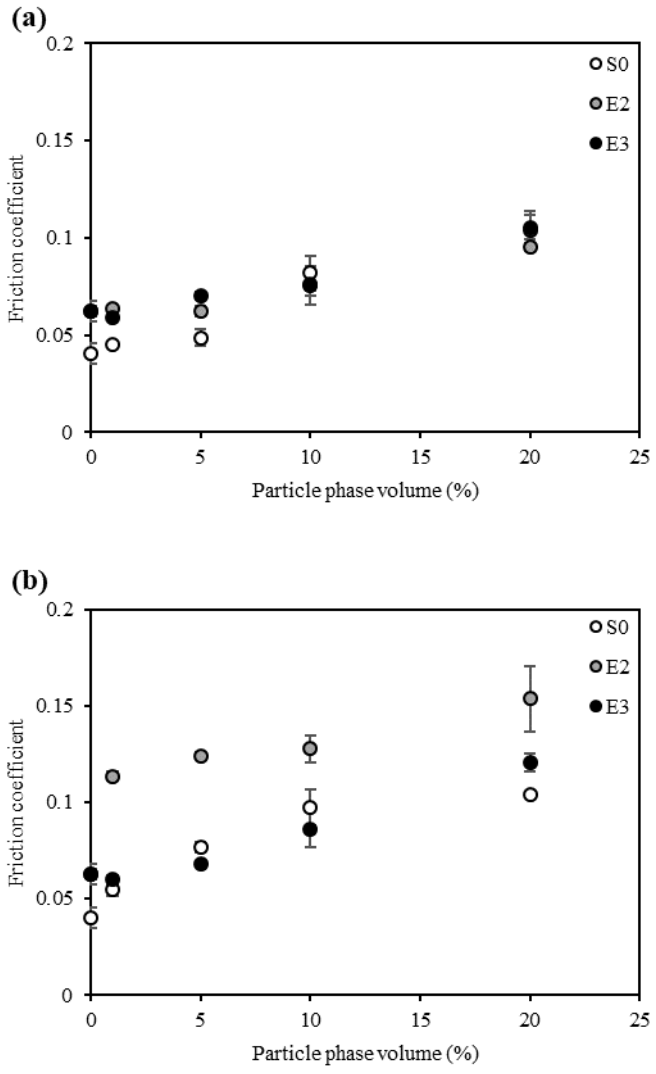

Figure 7 - friction coefficient at 750 mm/s versus particle phase volume for glycerol suspensions containing MCC particles sized 100-200 µm (a) and 500-700 µm (b) with surfaces S0, E2 and E3.

3.2.2. Soft particulate dispersions

The aim of these particular experiments was to further investigate the textured surfaces by examining agar fluid gels, which are deformable particulate suspensions irregular in shape. Agar concentrations of 2 and 4 wt% were examined. A tribopair of steel ball and PDMS discs were used with textures S0, E2 and E3 investigated.

The viscosity profiles of the agar fluid gels were measured (*Figure 8*). Shear viscosity increased upon raising agar concentration and both systems showed shear thinning behaviour as expected for particulate systems [37].

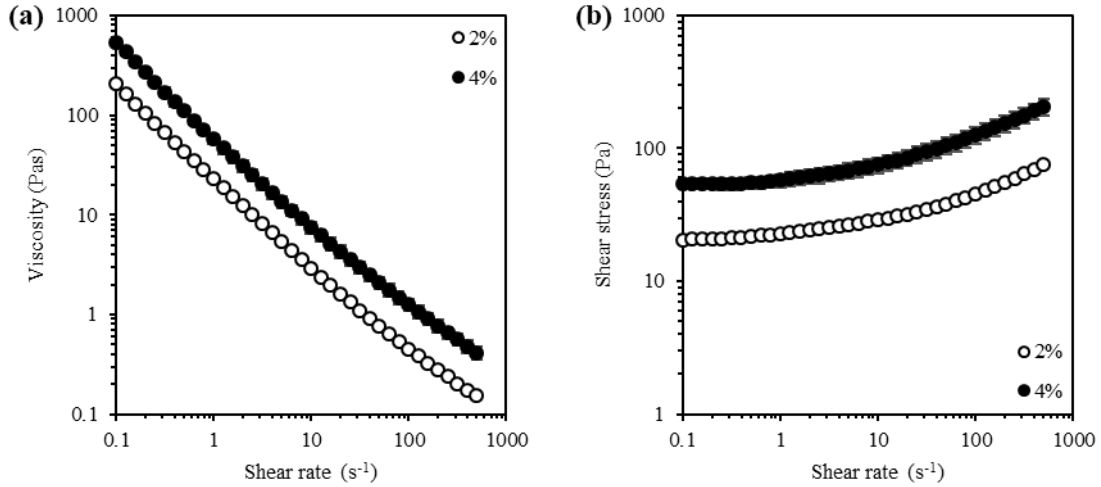

Figure 8 – shear rheology showing viscosity (a) and shear stress (b) as a function of shear rate for agar fluid gels of 2 and 4 wt%.

The friction coefficient of the agar fluid gels were measured (*Figure 9)* with surfaces S0, E2 and E3. The data collected from the agar fluid gel systems do not exhibit typical Stribeck behaviour. For all concentrations of agar, as speed increases to ~5 mm/s there was an increase in friction coefficient. This behaviour has been reported by Gabriele *et al.* where they attributed their observed increase in friction coefficient with entrainment speed due to particle exclusion of agarose fluid gel particles from the ball and disc contact with the continuous phase providing lubrication at low speeds [38]. These were larger than the magnitude of the roughness of soft surfaces used meaning the mixed regime passed a maximum friction coefficient before the speeds were great enough to generate a film

thickness that exceeds particle diameter, allowing entrainment and reducing friction. An alternative explanation is that at low speeds the agar fluid gels are entrained more efficiently and maintain a high viscosity film in the inlet region. Both of these explanations would need further study, and as suggested in other fluid gel studies, experiments using Surface Force Apparatus technique where the interaction forces between the two contacting surfaces are measured would help to elucidate the processes involved [28,39].

A lower maximum friction coefficient for textured surfaces E2 and E3 for 2% agar fluid gel was observed (*Figure 9a*). Here, particles are smaller than the cavities in E2 and E3. At low speeds, S0 shows the highest friction until speed increased and the mixed regime begins to transition to the EHL, during which the amount of particles entrained is expected to increase. It is proposed for these fluid gel systems, particles are able to fit inside the surfaces textures to reduce friction when the surfaces are in contact in the boundary and mixed regimes - which are said to be most relevant for oral processing [7]. Whereas for the smooth surface, particles were excluded from the contact until sufficient hydrodynamic pressure was achieved at higher speeds. At this point, for all surfaces, friction is similar and bulk properties of the fluid gel system dominate. For 4% agar fluid gel (*Figure 9b*), initially, S0 shows a greater friction coefficient compared to E2 and E3. As speed increases the surfaces behave similarly to one another whilst also exhibiting a lower friction coefficient compared to 2% agar, showing the contact is better lubricated by the more concentrated, more viscous fluid gel system, which is expected. The maximum friction coefficient for the surfaces was reduced for S0 from 0.6 to 0.45 and E3 from 0.5 to 0.4 as the concentration of agar increased. For surface E2, the maximum values were similar. With the greater concentration of agar, particle rigidity is expected to increase [40]. Greater lubrication by more rigid particles has been shown previously in Kappa-Carrageenan, agarose and alginate fluid gel systems where studies demonstrate that more rigid particles are able to support the normal load in the contact [28,38,41].

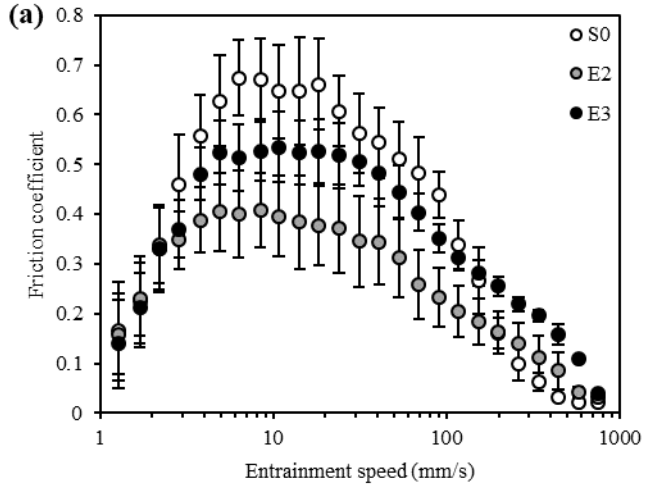

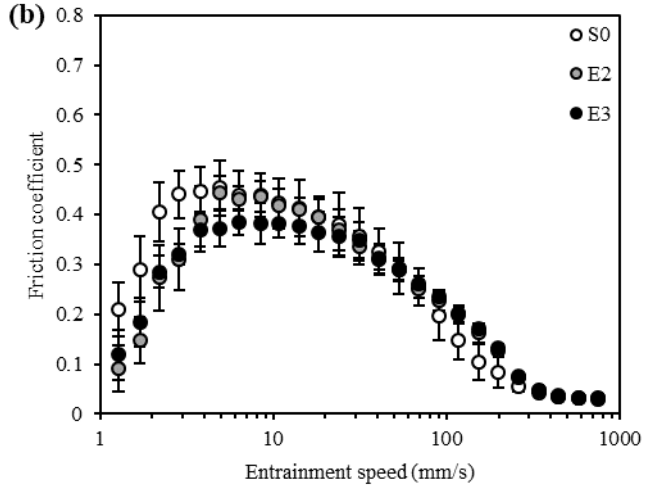

Figure 9 - friction coefficient versus entrainment speed for agar fluid gels at 2% (a) and 4% (b) agar concentrations with surfaces S0, E2 and E3.

4. Conclusions and future work

Textured surfaces were created by moulding and casting PDMS allowing the fabrication of a disc with cylindrical pillar cavities of a similar size to papillae found on the human tongue. Initially a system with Newtonian fluids was investigated using these textured discs. It was found the area density of pillars affected hydrodynamic lubrication, with a greater area density promoting full film lubrication. Specifically how the asperities alter the fluid hydrodynamics would require more work to visualise flow in the measurement gap. Furthermore, the textured discs were used to investigate particulate systems as it is common for food products to contain particles. Model hard, spherical particles showed

lower friction coefficients in the EHL regime so long as particles were smaller than the textures. Particles that were too large for the cavities increased friction. Soft, deformable particulate gels, commonly used in food products, demonstrated different behaviour to the 'model' particulate systems investigated where they showed lower friction in the mixed lubrication regime, which is suggested to be most relevant to oral processing. These results provide an insight into how particulate systems lubricate and interact with the surface in soft tribological contacts; which has relevance to oral processing applications as the tongue is not smooth like typical testing surfaces used in oral tribology. To understand particle and surface interactions further, a method allowing imaging and mapping of the soft contacts would be incredibly useful. Continued research is needed to link food formulations to physical properties, like friction, where closer resemblance to oral surfaces needs to be considered during experimental testing including surface chemistry and saliva effects.

5. References

[1] Spielman AI, Pepino MY, Feldman R, Brand JG. Technique to collect fungiform (taste) papillae from human tongue. J Vis Exp 2010. doi:10.3791/2201.

[2] Sarkar A, Andablo-Reyes E, Bryant M, Dowson D, Neville A. Lubrication of soft oral surfaces. Curr Opin Colloid Interface Sci 2019;39:61–75. doi:10.1016/J.COCIS.2019.01.008.

[3] Kullaa-Mikkonen A, Sorvari TE. A Scanning Electron Microscopic Study of the Dorsal Surface of the Human Tongue. Cells Tissues Organs 1985;123:114–20. doi:10.1159/000146050.

[4] Malone ME, Appelqvist IAM, Norton IT. Oral behaviour of food hydrocolloids and emulsions. Part 1. Lubrication and deposition considerations. Food Hydrocoll 2003;17:763–73. doi:10.1016/S0268-005X(03)00097-3.

[5] De Vicente J, Stokes JR, Spikes HA. Soft lubrication of model hydrocolloids. Food Hydrocoll 2006;20:483–91. doi:10.1016/j.foodhyd.2005.04.005.

[6] Laguna L, Farrell G, Bryant M, Morina A, Sarkar A. Relating rheology and tribology of commercial dairy colloids to sensory perception. Food Funct 2017;8. doi:10.1039/c6fo01010e.

[7] Stokes JR, Boehm MW, Baier SK. Oral processing, texture and mouthfeel: From rheology to tribology and beyond. Curr Opin Colloid Interface Sci 2013;18:349–59. doi:10.1016/j.cocis.2013.04.010.

[8] Godoi FC, Bhandari BR, Prakash S. Tribo-rheology and sensory analysis of a dairy semi-solid 2017. doi:10.1016/j.foodhyd.2017.04.011.

[9] Sonne A, Busch-Stockfisch M, Weiss J, Hinrichs J. Improved mapping of in-mouth creaminess of semi-solid dairy products by combining rheology, particle size, and tribology data. LWT - Food Sci Technol 2014;59:342–7. doi:10.1016/J.LWT.2014.05.047.

[10] Miao S, Lin D. Tribological analyses for the evaluation of food quality. Eval Technol Food Qual 2019:559–78. doi:10.1016/B978-0-12-814217-2.00021-4.

[11] Bongaerts JHH, Fourtouni K, Stokes JR. Soft-tribology: Lubrication in a compliant PDMS-PDMS contact. Tribol Int 2007;40:1531–42. doi:10.1016/j.triboint.2007.01.007.

[12] Dresselhuis DM, de Hoog EHA, Cohen Stuart MA, van Aken GA. Application of oral tissue in tribological measurements in an emulsion perception context. Food Hydrocoll 2008;22:323–35. doi:10.1016/j.foodhyd.2006.12.008.

[13] Yakubov GE, Branfield TE, Bongaerts JHH, Stokes JR. Tribology of particle suspensions in rolling-sliding soft contacts. Biotribology 2015;3:1–10. doi:10.1016/j.biotri.2015.09.003.

[14] Bongaerts JHH, Rossetti D, Stokes JR. The Lubricating Properties of Human Whole Saliva. Tribol Lett 2007;27:277–87. doi:10.1007/s11249-007-9232-y.

[15] Yashima S, Takase N, Kurokawa T, Gong JP. Friction of hydrogels with controlled surface roughness on solid flat substrates. Soft Matter 2014;10:3192–9. doi:10.1039/C3SM52883A.

[16] Cassin G, Heinrich E, Spikes HA. The influence of surface roughness on the lubrication properties of adsorbing and non-adsorbing biopolymers. Tribol Lett 2001;11.

[17] Krzeminski A, Wohlhüter S, Heyer P, Utz J, Hinrichs J. Measurement of lubricating properties in a tribosystem with different surface roughness. Int Dairy J 2012;26:23–30. doi:10.1016/j.idairyj.2012.02.005.

[18] Selway N, Chan V, Stokes JR. Influence of fluid viscosity and wetting on multiscale viscoelastic lubrication in soft tribological contacts †. | Soft Matter 2017;13:1702. doi:10.1039/c6sm02417c.

[19] Nguyen PTM, Nguyen TAH, Bhandari B, Prakash S. Comparison of solid substrates to differentiate the lubrication property of dairy fluids by tribological measurement 2016. doi:10.1016/j.jfoodeng.2016.03.026.

[20] Ranc H, Servais C, Chauvy PF, Debaud S, Mischler S. Effect of surface structure on frictional behaviour of a tongue/palate tribological system. Tribol Int 2006;39:1518–26. doi:10.1016/j.triboint.2006.01.017.

[21] Liu K, Tian Y, Stieger M, Van der Linden E, Van de Velde F. Evidence for ball-bearing mechanism of microparticulated whey protein as fat replacer in liquid and semi-solid multi-component model foods. Food Hydrocoll 2016;52. doi:10.1016/j.foodhyd.2015.07.016.

[22] Liu K, Tian Y, Stieger M, Van Der Linden E, Van De Velde F. Evidence for ball-bearing mechanism of microparticulated whey protein as fat replacer in liquid and semi-solid multi-component model foods. Food Hydrocoll 2016;52:403–14. doi:10.1016/j.foodhyd.2015.07.016.

[23] Chojnicka-Paszun A, De Jongh HHJ. Friction properties of oral surface analogs and their interaction with polysaccharide/MCC particle dispersions 2014. doi:10.1016/j.foodres.2014.05.028.

[24] Chojnicka-Paszun A, Doussinault S, De Jongh HHJ. Sensorial analysis of polysaccharide–gelled protein particle dispersions in relation to lubrication and viscosity properties. FRIN 2014;56:199–210. doi:10.1016/j.foodres.2013.12.035.

[25] Kim EHJ, Jakobsen VB, Wilson AJ, Waters IR, Motoi L, Hedderley DI, et al. Oral Processing of Mixtures of Food Particles. J Texture Stud 2015;46:487–98. doi:10.1111/jtxs.12157.

[26] Morell P, Chen J, Fiszman S. The role of starch and saliva in tribology studies and the sensory perception of protein-added yogurts. Food Funct 2017;8. doi:10.1039/c6fo00259e.

469 [27] Kieserling K, Schalow S, Drusch S. Method Development and Validation of Tribological
470 Measurements for Differentiation of Food in a Rheometer. Biotribology 2018;16:25–34.
471 doi:10.1016/J.BIOTRI.2018.09.002.

472 [28] Fernández Farrés I, Norton IT. The influence of co-solutes on tribology of agar fluid gels.
473 Food Hydrocoll 2015. doi:10.1016/j.foodhyd.2014.11.014.

474 [29] Lazidis A, Hancocks RD, Spyropoulos F, Kreuß M, Berrocal R, Norton IT. Whey protein fluid
475 gels for the stabilisation of foams. Food Hydrocoll 2016;53:209–17.
476 doi:10.1016/J.FOODHYD.2015.02.022.

477 [30] Sarkar A, Singh H. Oral Behaviour of Food Emulsions. Food Oral Process., Oxford, UK:
478 Wiley-Blackwell; 2012, p. 111–37. doi:10.1002/9781444360943.ch6.

479 [31] Sarkar A, Kanti F, Gulotta A, Murray BS, Zhang S. Aqueous Lubrication, Structure and
480 Rheological Properties of Whey Protein Microgel Particles. Langmuir 2017;33:14699–708.
481 doi:10.1021/acs.langmuir.7b03627.

482 [32] Pradal C, Stokes JR. Oral tribology: Bridging the gap between physical measurements and
483 sensory experience. Curr Opin Food Sci 2016;9:34–41. doi:10.1016/j.cofs.2016.04.008.

484 [33] Hertz H. On the contact of elastic solids. J Für Die Reine Und Ange- Wandte Math
485 1881;92:156–71.

486 [34] Wang X, Liu W, Zhou F, Zhu D. Preliminary investigation of the effect of dimple size on
487 friction in line contacts. Tribol Int 2009;42:1118–23. doi:10.1016/J.TRIBOINT.2009.03.012.

488 [35] Mourier L, Mazuyer D, Lubrecht AA, Donnet C. Transient increase of film thickness in micro-
489 textured EHL contacts. Tribol Int 2006;39:1745–56. doi:10.1016/J.TRIBOINT.2006.02.037.

490 [36] Andablo-Reyes E, Yerani D, Fu M, Liamas E, Connell S, Torres O, et al. Microgels as
491 viscosity modifiers influence lubrication performance of continuum. Soft Matter
492 2019;15:9614–24. doi:10.1039/c9sm01802f.

493 [37] Saha D, Bhattacharya S. Hydrocolloids as thickening and gelling agents in food: a critical
494 review. J Food Sci Technol 2010;47:587–97. doi:10.1007/s13197-010-0162-6.

495 [38] Gabriele A, Spyropoulos F, Norton IT. A conceptual model for fluid gel lubrication. Soft
496 Matter 2010;6:4205–13. doi:10.1039/c001907k.

497 [39] Israelachvili JN, McGuiggan PM. Adhesion and short-range forces between surfaces. part i:
498 New apparatus for surface force measurements. J Mater Res 1990;5:2223–31.
499 doi:10.1557/JMR.1990.2223.

500 [40] Gabriele A. Fluid gels: Formation, production and lubrication. The University of Birmingham,
501 2011.

502 [41] Garrec DA, Norton IT. The influence of hydrocolloid hydrodynamics on lubrication. Food
503 Hydrocoll 2012;26:389–97. doi:10.1016/j.foodhyd.2011.02.017.

504